IEEE ISIE 2006, July 9-12, 2006, Montréal, Québec, Canada

Hypersonic Electromagnetic Launch by Constant-Flux Synchronous Motor

Rainer B. Meinke[2], Daniel R. Kirk[1] and Hector Gutierrez[1]

[1]Department of Mechanical & Aerospace Engineering
Florida Institute of Technology, Melbourne, FL 32901

[2]Advanced Magnet Laboratory, Inc.
Melbourne, FL, 32901

Abstract. A novel concept for electromagnetic launching is presented. The propulsion system consists of a pulsed synchronous motor that generates a constant magnetic flux zone that moves with the projectile in a traveling wave. The cylindrical projectile is equipped with high-temperature superconducting coils in persistent mode, charged prior to launch. The current pulses supplied to the track coils are adjusted in time (leading and trailing edge, pulse duration, pulse frequency) so that no magnetic flux change is seen by the superconducting coils as the projectile moves during launch. Constant flux translates to no voltage or additional currents being induced, which prevents the projectile coils from quenching or overheating. The projectile coils, built in a cable-in-conduit assembly as in pulsed fusion magnets, can carry persistent currents of up to 50 kA under severe operating conditions in pulsed magnetic fields with no need for induction or external power supply. The proposed constant flux synchronous motor (CFSM) is self-centering and avoids mechanical contact between the track and the projectile - the electromagnetic forces and torques are sufficient to compensate for the aerodynamic disturbance forces and moments during launch. A low pressure helium atmosphere inside of the launch tube is also proposed, which nearly eliminates both aerodynamic and heat transfer effects (forces, torques and heating) due to high speed gas flow around the projectile, with large safety margins. The proposed technology removes several of the technical problems that made hypersonic electromagnetic launch unfeasible, in particular the inductive heating of the projectile when a contact-free armature is desired.

1. Introduction

Electromagnetic (EM) launching has been pursued in the last three decades as an efficient and economical alternative to chemical propulsion for military and aerospace applications. Although several different concepts have been proposed, a number of unresolved technical challenges have prevented it from becoming a reality. Broadly speaking, the critical limitations of EM launching have been (i) large heat dissipation, leading to potential damage to both payload and launcher when reaching high speeds, (ii) complex wear and contact phenomena resulting from mechanical contact at high speeds, (iii) the lack of an efficient method to generate current in the projectile without excessive heating of the payload.

This paper presents the constant-flux synchronous motor (CFSM), a novel concept that addresses most of these critical problems. The CFSM launcher is based on a constant magnetic flux zone that moves with the projectile in a traveling wave. Constant-flux operation eliminates inductive heating of the projectile. Superconducting rings operating in persistent mode are used as current source in the projectile, eliminating the need of feeding the launch vehicle through brushes, contact armatures or AC induction. The resulting contact-free, self centering suspension and propulsion dramatically improves survivability (wear and tear) of the launcher since heat dissipation in the track during launch is relatively small and distributed over the length of the launcher. A conical/cylindrical projectile design allows stabilization by spinning, introduced at the home position prior to launch- this stabilizes the projectile both during the acceleration phase and during the coasting flight through the atmosphere. There is no need for detachable sabot or other parasitic mass – the effective launch mass can be 100 %. For these reasons, the CFSM can be a breakthrough concept for both direct EM launch to orbit and EM kinetic kill weapons.

2. Description of the CFSM Launch Tube Concept

The rail gun is the EM launch technology that has received the most attention in recent years. Rail guns have several attractive characteristics but also some unresolved challenges, mostly given by the complex contact phenomena between rails and armature at very high speeds, as well as the significant heat dissipation associated to each launch, which results in damage to the gun's insulation that substantially limits the rate of fire and the overall survivability of the gun. Coaxial induction launchers have some desirable advantages over other EM launch methods in that no direct electrical contact is required, but pulsed induction motors or coil guns that can provide the required thrust force for hypervelocity applications would need to induce very large currents in the projectile - the resulting ohmic losses would lead to unmanageable heat loads and thermal destruction of the projectile.

The "Constant Flux Synchronous Motor" (CFSM) delivers the required propulsion forces without inducing any significant eddy currents in neither projectile nor launch vehicle. To avoid inducing significant eddy currents, the projectile coils have to see an almost constant magnetic flux during launch, a requirement that has never been met in any existing system. The CSFM launch system consists of the following components:

1-4244-0497-5/06/$20.00 © 2006 IEEE

a) Normal conducting coils on the stationary track, pulsed with 30 to 100 kA during launch depending on the number of turns in the windings. The pulses are synchronized with the moving projectile by an appropriate hardware trigger. Near-constant flux seen by the projectile is essential to the CFSM concept. A change in flux in the projectile's coils would induce a voltage that would create eddy currents in the coil's substrate. The resulting ohmic heating could quench or even destroy the projectile's coils.

b) Superconducting coils on the projectile, operated in persistent mode (30 to 50 kA, depending on the number of turns). The coils are inductively charged prior to launch - no additional power is needed to maintain the DC currents in the projectile coils.

c) Independent pulsed power supplies connected to the launch track coils. Current in the launcher coils follow programmed pulse shapes (rise time, fall time and pulse duration) triggered by the position of the projectile along the track. The shape of the current pulses is calculated off-line - they depend on the instantaneous geometric relationship between track and projectile coils. The pulsed power supplies can be implemented as 2 or 3 combined Marx generators charged with individually controlled voltages and discharged with individually controlled delays for each track coil, in a way that pulse shapes can be adjusted to the required waveforms.

d) An energy storage system with sufficient storage capacity and power rating. There are several qualified technologies that could be used (e.g., batteries, capacitors or superconducting magnetic energy storage devices). Since the heat dissipation is substantially smaller than in other EM technologies, and the effective mass fraction can be 100%, the energy and power requirements are advantageous compared to other EM launch technologies.

Conventional coaxial launchers rely on either external power supplies that feed the projectile through brushes, or induced eddy currents. These technologies have inherent limitations in the maximum speeds they can provide. In a DC coaxial launcher this is given by the wear and contact phenomena in the projectile's brushes, as well as ohmic heating of the projectile. In an induction launcher, inductive heating of the projectile is a limiting factor.

In a conventional pulsed coil gun, the change in speed of the projectile during launch is accommodated by increasing either pole pitch or input frequency or both along the track. In the CFSM, the sequence of pulses supplied to the track coils forms a traveling wave that determines the speed of the projectile. Since there are no iron cores in the system, the pulse shapes required to produce constant flux as seen by the projectile coils depend solely on the geometric relationships of track and projectile and can be analytically calculated off-line.

2.1 CFSM Launch Track Layout

The interaction between the track and projectile coils provide the required propulsion forces as well as self-centering suspension forces. Projectile stabilization during launch is achieved both by the self-centering action of the electromagnetic forces and by spinning the projectile prior to launch. The use of a low pressure environment in the track will minimize drag and heat transfer during launch. The schematic layout of the CFSM launcher is shown in Figure 1. The basic cell of the launch tube consists of M "rear" coils (T_{R1}, T_{R2}, ... T_{RM}) and M "front" coils (T_{F1}, T_{F2}, ... T_{FM}). The "rear" coils of such a section are pulsed with opposite current direction than the "front" coils. The distance between track coils P_T is the distance where $\frac{\partial M}{\partial x}$ (the gradient of M with respect to x) is maximum. This is calculated off-line and depends only on the launcher geometry.

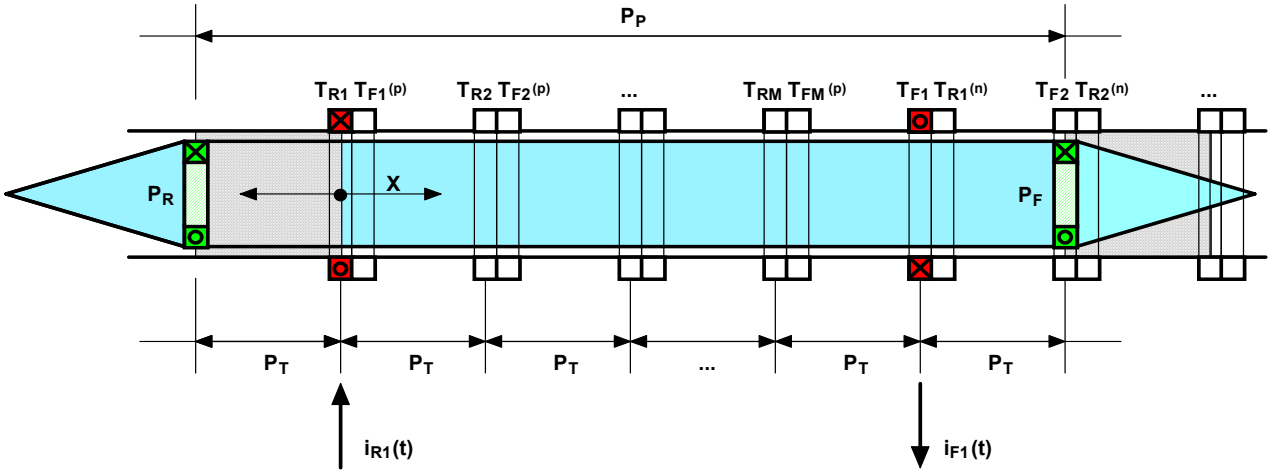

Figure 1: A longitudinal section of the CFSM launcher. P_B: Basic cell length of CFSM system = $2\,M \times P_T$, for some integer M. The distance between the rear coil T_{R1} and the corresponding front coil T_{F1} is $M \times P_T$. P_P: distance between coils in the projectile, P_T: distance between coils in the track. Superindexes *(p)* and *(n)* denote coils of the *previous* and *next* track sections to be fired.

The force between the projectile coil P and the track coil T is given by: $F = i_P i_T \frac{\partial M}{\partial x}$. The force is attractive when both currents are in the same direction and repelling when the currents have opposite directions. While the projectile coils are repelled from the nearest (active) track coil, the current pulse in the track coil increases in such a way that it keeps the magnetic flux seen by the projectile approximately constant until the projectile reaches the next track coil. At this moment in time the current pulse in the active track coil rapidly goes to zero and the next track coil is pulsed in such a way that the flux through the projectile stays (approximately) constant. Synchronization is achieved by hard-wiring the firing circuits of individual energy storage elements to sensors that detect the position of the projectile along the launch tube. In Figure 1:

- The projectile coil currents i_{PR} and i_{PF} are constant (persistent mode superconducting currents) and both have the same current direction.

- Each track coil is connected to an independent pulse power supply which is able to supply a pre-determine pulse shape. Only two track coils are ON at any given time. In the picture, T_{R1} and T_{F1} (in red) are currently being pulsed. Triggering the track coils is hardware-controlled by proximity switches that detect the presence of the projectile.

- The "rear" pulse $i_{R1}(t)$ starts when the projectile coil P_R reaches $x = -P_T$ and ends when P_R reaches $x = 0$. The coordinate x is relative to the coordinate system that moves with the projectile. Similarly, the "front" pulse $i_{F1}(t)$ is only ON while the front projectile coil P_F is traveling through the front shaded area. The current pulses $i_{R1}(t)$ and $i_{F1}(t)$ are calculated off-line as described in the next Section. The rear coil pulls the projectile to the right (currents in the same direction) while the front coil pushes it to the right (currents have opposite directions).

- After a section is fired, the next section starts ($T_{R1}^{(n)}$, $T_{R2}^{(n)}$, ...). Notice that the "front" coils of the previous section fired are placed in close proximity to the "rear" coils of the current section (T_{R1} with $T_{F1}^{(p)}$, T_{R2} with $T_{F2}^{(p)}$, ..., and also $T_{R1}^{(n)}$,with T_{F1}, $T_{R2}^{(n)}$*with* T_{F2}, etc.).

- For a slender projectile (i.e. length >> diameter), it is assumed that the effect of a "front" track pulse on the rear shaded section is negligible. Similarly, the effect of the "rear" track pulse on the front shaded section is negligible too.

- The mutual inductance $M(x)$ between the projectile coil and the track coil that are interacting at any given moment (in the picture, *PR* with T_{R1}, and *PF* with T_{F1}) is a function of the instantaneous axial position "x" and the basic launcher geometry (launcher diameter, projectile diameter, and air gap). Since there are no iron cores, $M(x)$ is easily and accurately calculated off-line.

Coils T_{R1} and T_{F1} are fired at the same time, when $x = -P_T$. When $x = 0$, T_{R1} and T_{F1} are turned OFF. The origin of the coordinate system "X" moves to T_{R2}. At the same time, the pulses in T_{R2} and T_{F2} start. Again, the "rear" currents are fired in the same direction as the projectile current, whereas the "front" coils are fired in opposite direction. This way, the rear coil is always pulling the projectile forward while the front coil is pushing. T_{R2} and T_{F2} are turned OFF when the local coordinate x reaches zero. The sequence is repeated until the last coils of the section T_{RM} and T_{FM} are fired. The next section ($T_{R1}^{(n)}$ and $T_{F1}^{(n)}$, $T_{R2}^{(n)}$ and $T_{F2}^{(n)}$, ...) fires in similar manner. Notice that the coils in the "front" section always fire in direction opposite to the projectile coil currents, and so on. If a given pulse shape is difficult to achieve with a single pulse source or Marx generator, two or three can be operated in parallel to obtain the required pulse shape by superposition. Some pulse characteristics (i.e. rise time) are given by track parameters such as number of turns (i.e., inductance) of a given coil.

2.2 Analytical Overview of the CFSM Concept

As described in the previous section, the only track coils active at any given time are the two located immediately ahead (T_{R1}) and immediately behind (T_{F1}) of the projectile rear and front coils, respectively. The corresponding current pulses last only while coils P_R and P_F are moving within their corresponding shaded areas. The time taken to travel the shaded subsection P_T is t_{PT}.

The magnetic field and flux acting on the projectile coils P_R and P_F while traveling within the shaded areas will be considered. A simpler case will be analyzed first: pitch and yaw angles are assumed to be small, and the centers of coils P_R and P_F are considered near the axis of symmetry of the launch tube. In this case, the magnetic field B produced by the track coils T_{R1} and T_{F1} on any circular concentric path within the surfaces enclosed by P_R and P_F has cylindrical symmetry (i.e., B is the same for all points along any concentric circular path within the surfaces enclosed by P_R and P_F). The flux ϕ caused by the track coil T_{R1} on the surface enclosed by P_R can therefore be calculated using circular differential elements as shown in Figure 2.

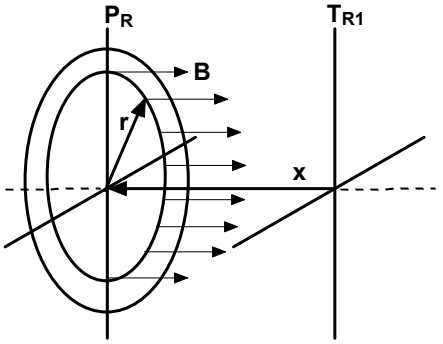

Figure 2 - Magnetic Flux through a Projectile Coil section.

The flux ϕ caused by the track coil T_{R1} on the surface enclosed by P_R is: $\phi = \int_A BdA \cong \sum_{k=0}^{N} B(2\pi k\Delta r)\Delta r$, where B is some nonlinear function of the geometry and the current i_{R1}, $B = i_{R1}g(r,x)$, and $r = k\Delta r$ is the discretized version of the continuous variable r. The index k numbers the concentric rings used in this numerical approximation. The field of the projectile coil P_R is not included on the flux calculation since it's a stationary constant field that travels with the projectile and therefore causes no induction $\varepsilon = -d\phi/dt$ on the projectile's coil. The condition for near-constant flux on the projectile coil P_R traveling in the rear shaded area of Figure 1 can now be written as:

$$2\pi\sum_{k=0}^{N} i_{R1}(t)g(k\Delta r,x)(k\Delta r)\Delta r + 2\pi\sum_{k=0}^{N} i_{F1}(t)g(k\Delta r,x+MP_T)(k\Delta r)\Delta r = \Phi_0 \quad (1)$$

which includes the effect of the two track coils being pulsed (T_{R1} and T_{F1}, with currents $i_{R1}(t)$ and $i_{F1}(t)$) on the rear projectile coil P_R. $M\times P_T$ is the distance between coils T_{R1} and T_{F1} (the length of a basic track section is $2M\times P_T$) and Φ_0 is some characteristic flux to be kept near constant. For a slender projectile (i.e., the projectile radius R_P is much smaller than the length of the half-section $M\times P_T$), this can be simplified by neglecting the effect of the front track coil T_{F1} (which is rather far away) on the rear projectile coil P_R:

$$2\pi\sum_{k=0}^{N} i_{R1}(t)g(k\Delta r,x)(k\Delta r)\Delta r \cong \Phi_0, \quad -P_T < x < 0 \quad (2)$$

and $\Delta r = \frac{R_P}{N}$, where N is an arbitrarily large integer. This can be regrouped as:

$$\sum_{k=0}^{N} i_{R1}(t)g(k\frac{R_P}{N},x)k \cong \frac{\Phi_0}{2\pi\left(\frac{R_P}{N}\right)^2}, \quad -P_T < x < 0 \quad (3)$$

The time taken to travel the shaded subsection (t_{PT}) is discretized as $t = j\Delta t$, where $\Delta t = \frac{t_{PT}}{M_t}$ and M_t is some (large) integer, $j=0 \ldots M_t$. The required current pulse $i_{R1}(t)$ at time $t = j\Delta t$, must meet the near-constant flux condition (3):

$$\sum_{k=0}^{N} i_{R1}(j\Delta t)g\left(k\frac{R_P}{N},x(j\Delta t)\right)k \cong \frac{\Phi_0}{2\pi\left(\frac{R_P}{N}\right)^2}, \quad -P_T < x < 0 \quad (4)$$

where $x = x(j\Delta t)$ is the position of the projectile coil P_R relative to the coordinate system T_R at the present moment. In this expression, the required current pulse $i_{R1}(t)$ does not depend on the integration variable k, and can therefore be factored out of the summation above. This yields:

$$i_{R1}(j\Delta t) \cong \frac{\Phi_0}{2\pi\left(\frac{R_P}{N}\right)^2\sum_{k=0}^{N} g\left(k\frac{R_P}{N},x(j\Delta t)\right)k} \quad (5)$$

for $-P_T < x < 0$, which illustrates how the desired current pulse $i_{R1}(t)$ is a function of the instantaneous position $x = x(j\Delta t)$, and $g(r,x)$, that depends on the geometric relationship of track and coil. The current $i_{R1}(t)$ and the position $x = x(j\Delta t)$ are related in this model through Newton's second law and the electromagnetic thrust forces:

$$F_x = m\ddot{x} \approx i_{R1}(t)i_{PR}\left.\frac{\partial M}{\partial x}\right|_x + i_{F1}(t)i_{PR}\left.\frac{\partial M}{\partial x}\right|_{2P_T+x} \quad (6)$$

for $-P_T < x < 0$, where m is the projectile's mass, i_{PR} is the projectile coils current (a constant) and the gradient $\frac{\partial M}{\partial x} = f(x)$ can be calculated off-line and interpolated as a function of the projectile's position x. In the launch tube's low-pressure atmosphere the aerodynamic drag can be neglected and therefore the total force in the x direction is determined by the electromagnetic thrust forces. The dynamic dependence of current, force and position can be described by converting the algebraic condition (5) into a differential condition in time. Taking the derivative of Equation (3) with respect to time, yields, for $-P_T < x < 0$:

$$\sum_{k=0}^{N}\frac{di_{R1}(t)}{dt}g(r,x)k + \sum_{k=0}^{N} i_{R1}(t)\left(\frac{\partial g}{\partial r}\dot{r} + \frac{\partial g}{\partial x}\dot{x}\right)k = 0 \quad (7)$$

where $r = k\frac{R_P}{N}$. A similar equation can be written for the front coil current $i_{F1}(t)$. Since both $i_{R1}(t)$ and its time derivative are independent of the summation variable k, this equation can be rearranged as follows:

$$\frac{di_{R1}(t)}{dt} = -i_{R1}(t)\frac{\sum_{k=0}^{N}\left(\frac{\partial g(k\frac{R_P}{N},x)}{\partial x}\dot{x}\right)k}{\sum_{k=0}^{N} g(k\frac{R_P}{N},x)k} \quad (8)$$

where the projectile speed is large ($\dot{x} >> \dot{r}$) and therefore the term $\frac{\partial g}{\partial r}\dot{r}$ in (7) can be neglected.

The corresponding expression for the front coil is:

$$\frac{di_{F1}(t)}{dt} = -i_{F1}(t)\frac{\sum_{k=0}^{N}\left(\frac{\partial g(k\frac{R_P}{N},2P_T+x)}{\partial x}\dot{x}\right)k}{\sum_{k=0}^{N} g(k\frac{R_P}{N},2P_T+x)k} \qquad (9)$$

Equations (6), (8) and (9) define the dynamic relationship between the track pulses $i_{R1}(t)$, $i_{F1}(t)$ and the projectile's motion. The coupled equations can now be described as a system of four nonlinear ordinary differential equations of the four state variables:

$$z_1(t) = i_{R1}(t), \quad z_2(t) = i_{F1}(t), \quad z_3(t) = x, \quad z_4(t) = \dot{x}$$

$$\frac{d\vec{z}}{dt} = \vec{F}(\vec{z},t) \qquad (10)$$

$$\begin{bmatrix} dz_1/dt \\ dz_2/dt \\ dz_3/dt \\ dz_4/dt \end{bmatrix} = \begin{bmatrix} -z_1 z_4 \dfrac{\sum_{k=0}^{N}\left(\frac{\partial g(k\frac{R_P}{N},z_3)}{\partial z_3}\right)k}{\sum_{k=0}^{N} g(k\frac{R_P}{N},z_3)k} \\ -z_2 z_4 \dfrac{\sum_{k=0}^{N}\left(\frac{\partial g(k\frac{R_P}{N},2P_T+z_3)}{\partial z_3}\right)k}{\sum_{k=0}^{N} g(k\frac{R_P}{N},2P_T+z_3)k} \\ z_4 \\ z_1\frac{i_{PR}}{m}\frac{\partial M}{\partial z_3}\Big|_{z_3} + z_2\frac{i_{PR}}{m}\frac{\partial M}{\partial z_3}\Big|_{2P_T+z_3} \end{bmatrix} \qquad (11)$$

The coupled system of ordinary differential equations (11) can be readily solved using standard numerical techniques such as the Runge-Kutta-Fahlberg or Adams-Moulton algorithms, starting at the initial conditions:

$$z_1(\varepsilon) = i_{\max}, \quad z_2(\varepsilon) = Gi_{\max}, \quad z_3(\varepsilon) \approx -P_T, \quad z_4(\varepsilon) \approx \dot{x}_0 \qquad (12)$$

where ε is the (hardware given) shortest time in which the energy storage devices can discharge the maximum current peak i_{max}, and $\dot{x}_0$ is the projectile velocity at the end of the previous track segment (ε is typically very small compared to the total duration of the pulse t_{PT}). The numerical solution of (11) subject to (12) ends when $z_3 = 0$, yielding the current waveforms $i_{R1}(t)$, $i_{F1}(t)$ that generate maximum thrust in the launch vehicle while keeping a near-constant flux region that travels synchronously with it. Notice that for the rear coil solution, the initial condition is $i_{R1}(\varepsilon) = i_{max}$, whereas for the front coil $i_{F1}(\varepsilon) = G\, i_{max}$ where $0 < G < 1$ is a constant to be optimized by successive solutions of (11) subject to (12).

2.3 Persistent Current Superconducting Coils

The projectile will have two superconducting coils (rings) as shown in Figure 3. The projectile could be launched as a single piece (no separation required after launch) or could detach after launch from some of its mass, if needed for some application such as serving as first stage for a laser propulsion engine (Figure 3 (a)).

The superconductor in these rings is in short circuit, to form a DC current path with almost zero resistance. The rings are charged inductively prior to launch. The individual superconducting wires or tapes are inserted in a robust metallic conduit, filled with the cryogen (most likely helium or hydrogen) to cool the superconductor to the required operational temperature. Prior to launch, these rings would be connected via umbilical cords (small cryogenic transfer lines) to a refrigerator, and cooled to the operational temperature. The umbilical cords are disconnected shortly before the launch, and the superconductor is kept at the operational temperature by the amount of cryogen inside of the conductor conduit. Since the duration of launch is about 0.5 seconds and the aerothermal heating is estimated to be about 50 K in a low pressure environment, a modest amount of cryogen is sufficient to keep the conductor in the superconducting state. Considering this, the cryostat surrounding the superconductor, which typically consists of a vacuum vessel and thermal radiation shield, can be simple and inexpensive for this application.

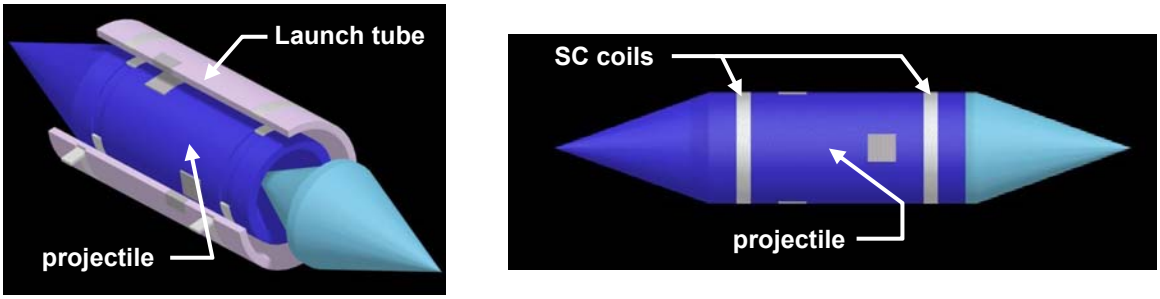

Figure 3: a) Layout of projectile inside a section of the launch tube, when used as first stage to launch a laser propulsion engine. b) Projectile with superconducting rings

The technology of placing LTS superconductors in metallic conduits has been well developed for pulsed fusion magnets. Due to the direct contact between the superconductor and the cryogen in this cable-in-conduit technology, energy deposition from pulsed magnetic fields or conductor displacement is absorbed by the cryogen. A typical superconductor with a current carrying capacity of about 50 kA is shown in Figure 4.

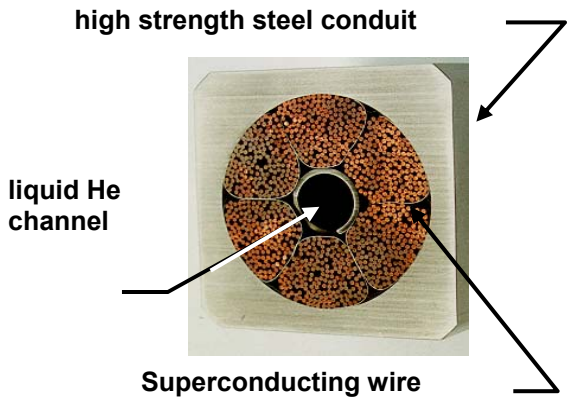

Figure 4: Cable-in conduit used on the ITER CS Model Coil. The conduit dimensions are ~ 50x50 mm. This CICC conductor operated successfully at 46 kA and 13 Tesla, at a magnetic field pulse rate of 2 Tesla/sec.

BSCCO, YBCO and MgB_2 high temperature superconductors (HTS) are already available in wire and tape form. If operated at temperatures below 20 K, these conductors can carry large currents at rather high magnetic fields. BSCCO-2212, and MgB_2 operated at 4.5 K, have a much higher critical field than any low temperature superconductor (LTS). While not absolutely necessary for the proposed launcher application, HTS conductors would offer a much higher energy margin and therefore quench safety than LTS conductors. The amount of heat that can be accommodated in HTS conductors can exceed those of LTS by a factor of several thousand. This large energy margin is due to the much higher enthalpy of materials at higher temperature and the much larger gap between operational temperature and critical temperature. HTS superconductors, operating at 20 to 30 K, offer a much higher safety margin between nominal operation and quench than low temperature superconductors operating at liquid helium temperatures (typically 4.5 K).

3. Aerodynamic and Aerothermal Effects

The aerodynamics and heat transfer calculations for the sled/projectile while contained within the launch tube have been performed using both closed-form analytical solutions as well as using numerical calculations. In an evacuated launch tube (~ $1/100^{th}$ of an atmosphere) the aerodynamic forces, i.e. lift, drag and moments, are within manageable levels and can easily be compensated by the electromagnetic forces. For example, lift and drag are on the order of 1-15 kN and the moments at maximum misalignment of the projectile allowed by the launch tube geometry are ~ 20 kN m. A parametric study has been performed over a range of Mach numbers and vehicle orientations. These results are to be integrated with the coupled electromagnetic-dynamics simulation currently being developed in Simulink.

Although aerodynamic forces and moments are easily overcome by magnetic forces within the launch tube at relatively modest vacuum levels, it has been found that the $1/100^{th}$ of an atmosphere vacuum is essential to alleviate heat transfer concerns within the launch tube. Using stainless steel as the sled material, a series of simulations were conducted to ensure that the material would not approach melting temperatures. The studies were performed by evaluating the heat flux along the surface of the projectile during a 0.5 second simulated acceleration from zero to 7 km/s. Even using worst case constant heat flux, it was found that the surface temperature of the stainless steel projectile body would only increase by about 50 °C if the pressure within the launch tube were kept to $1/100^{th}$ of an atmosphere. Thus the preliminary studies indicate that the level of vacuum required is governed by heat transfer considerations rather than the need to minimize aerodynamics disturbance forces within the launch tube. The heat transfer within the launch tube is currently being investigated using computational methods coupled to the flow solution.

Although the aerodynamic heating within the launch tube does not present a significant challenge (due to the low pressure and density of the gas) the heating of the projectile upon exit of the launcher into the dense ground-level atmosphere is an issue that must be thoroughly examined before a definitive statement on the feasibility of direct launch from the surface of the Earth to orbit can be made. For example, the projectile must be able to tolerate extremely large heat fluxes for 10-15 seconds as the vehicle travels at around 7 km/s through the dense lower atmosphere. Numerous studies have indicated that flyout velocities of around 6.5 km/s are feasible from a heat transfer perspective [1,2]. Furthermore, these references indicate that at these speeds, “Sea level launch poses no unusual difficulty”, [2]. Although these sources indicate that such launch speeds are feasible, experimental validation, especially using ablative techniques, has not been completed. Work has begun on exploring appropriate analytical, numerical, and experimental techniques for assessing the performance of the vehicle as it travels through the dense portion of the atmosphere at extremely high speeds and experiences heat fluxes on the order of several ten kW/cm^2. A significant effort should also go to optimizing the shape of the projectile, examining various surface ablator materials (such as plasma sprayed tungsten which has recently been perfected), and the use of novel multi-layer aerodynamic shells to withstand the high heat loads. Numerical efforts will be explored to complement other work currently sponsored by AFOSR.

4. Experimental Qualification of the CFSM Concept

The constant-flux principle is based on the static relationships of current-field-flux given by the geometric relationships between track coils and projectile coils. Therefore the principle can be tested under semi-static conditions (low speed). Figure 5 shows a section of a test set-up used to demonstrate the constant-flux principle.

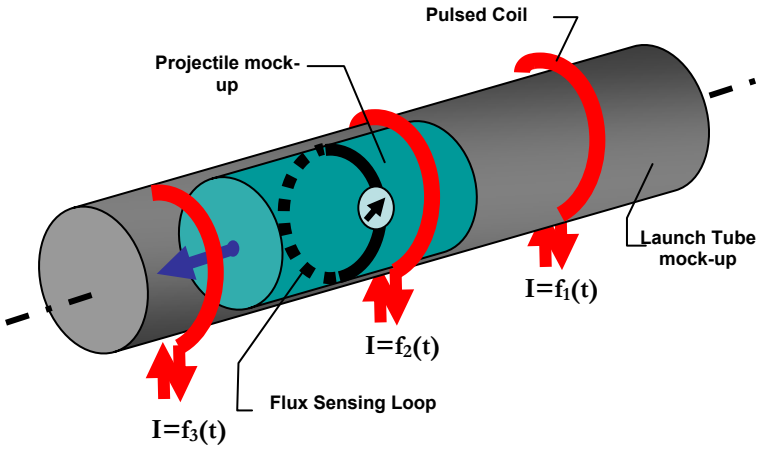

Figure 5: Linear test rig for qualification tests of the CFSM system.

The linear test rig represents a section of the launch tube with a few track coils implemented. A projectile mock-up will be moved along the tube to trigger the sequence of current pulses $f_1(t)$, $f_2(t)$, $f_3(t)$. The mock-up projectile is rigged with a flux sensing coil - any flux change experienced by the test coil would induce a voltage that can be externally measured. Integrating the signals from the flux sensing loops measures the total flux change seen by the test coil. The projectile mock-up can be moved to any position relative to the pulsed track coils, and the current waveforms calculated by solving (11) subject to (12) can be generated by computer-controlled current sources. Applying the calculated pulse shapes to the mock-up track coils and measuring the induced voltage simulates the flux seen by the coil on the moving projectile. Flux measurements as a function of time will be performed for all positions between two track coils. For a correctly shaped current pulse, the measured voltage and therefore the flux should be constant at all test positions.

The tests will show what level of accuracy in pulse-shaping is needed to experience acceptable flux changes in the actual system, or otherwise, which flux changes will be seen by the moving projectile coils for a given inaccuracy in the actual pulse shape. These tests and the corresponding calculations will help optimize the CFSM system, and estimate the induced voltages (and therefore parasitic currents) induced in the moving projectile as a result of non-ideal pulse shaping. While it is in principle possible to adjust the pulse shapes to any level of accuracy, system complexity, robustness and cost suggests the use of the simplest pulse power system that will not cause quenching and overheating of the projectile coils. Various coil configurations for track and projectile can be tested and compared with calculations. The linear test rig could also be used to measure the propulsion and levitation forces, using active coils in the projectile mock up. Since the mock-up would only move over short distances, external connections for the coils would be easy to implement.

4.1 Superconductor Qualification Tests

Quench Stability. A prototype coil consisting of a few turns of superconductor would be excited to the required operational current. A second coil in close proximity would be used to simulate the flux changes that are expected in actual operation of these coils. Inducing flux changes of various levels into the prototype projectile coil, its quench stability can be tested. The flux changes used in these tests can be stronger than expected in the actual system to guarantee a sufficient operational margin during actual operation.

Mechanical Stability. During launch, the superconductor in the projectile coil will experience significant mechanical forces due to inertial acceleration. Superconductors (either LTS or HTS) have never been tested under such conditions. The inertial acceleration is equivalent to compression of the conductor, i.e., the mechanical launch conditions can be simulated by compressing the conductor. To test stability to mechanical stress, the conductor would be placed in a cryostat with a background field of appropriate strength that simulates the self-field of the projectile coil and the field due to the track pulses. The conductor is then loaded to the appropriate mechanical pressure and its critical current measured. The conductor and its enclosure should pass these tests without quench with at a significant safety margin. These tests can be performed with different superconductors to identify the best choice.

4.2 Nose Cone Ablation

Coasting flight of the projectile through the atmosphere remains a major issue and requires special testing. High intensity particle beams, as used on electron beam welding, produce sufficient heat flow densities to simulate the effects of low-altitude atmospheric coasting on the projectile. The study of hypersonic launch from ground requires an ablation study using nose cones of various designs and materials at a test beam facility.

It seems feasible to use experimental methods to investigate the high heat fluxes originated by atmospheric coasting from ground by making use of electron beam welding techniques, which can produce surface heat fluxes as high as 10^3-10^6 kW/cm^2 [3]. Although the actual physical situation between shear layer heating during atmospheric flight and electron beam penetration to achieve the heat flux is quite different, exposing various nose cone geometries or cooling techniques to these intense heat loads will

nonetheless provide valuable guidance for the design of the actual projectile.

If the vehicle can withstand the high heat loads during the initial ascent (first several seconds), the heat flux then monotonically decreases to much more tolerable levels (2-5 kW/cm^2). Current research suggests that, *"Lightweight flexible phenolics, such as PhenCarb-28 at 28 lb/ft^3, look promising for [planetary exploration] missions with peak heating in the range from about 1,000 to 2,000 Btu/ft^2-sec (~1.1 to 2.3 kW/cm^2). A Phencarb-32 or -36 should have more optimal performance and efficiency for still higher heating"*, [4]. The existing arc-heated facility -NASA MSFC PRL- is capable of producing heat fluxes on the order of 0.5 kW/cm^2, so heat transfer experiments simulating the vehicle at times after flight through the densest portions of the atmosphere (after the first 1-5 seconds) can be readily accomplished.

Another option includes plasma sprayed high-temperature refractory metals and ceramics. For example, *"Ultramet has developed and repeatedly demonstrated a refractory ceramic coating material capable of non-ablating, long-term operation (minutes to tens of minutes) under air arcjet conditions at heat flux and enthalpy levels, simulating leading edge reentry conditions, of 350 Btu/ft^{2}sec (~0.4 kW/cm^2) and 12,000 Btu/lbm respectively. This unique material has also survived heat flux levels as high as 800 Btu/ft^{2}sec (~1 kW/cm^2), without erosion, under lower enthalpy conditions. This patented coating material, designated Ultra2000, is composed of fine alternating layers of hafnium carbide (HfC) and silicon carbide (SiC), applied by chemical vapor deposition (CVD), to a total thickness of just 0.005-0.010". Ultra2000 is capable of long-term, non-ablating operation at surface temperatures as high as 4000ºF, and has been effectively applied to and tested on various ceramic matrix composites, carbon-carbon composites, and graphite substrates",* [5].

In summary, it appears that if the vehicle can survive the intense heat fluxes for the first few seconds of launch (1-3 seconds to arrive at 16,000 km, where the atmospheric density has already dropped significantly), proven thermal protection systems are then available to protect the projectile for the remainder of the flight. These options should be further studied to develop and test an appropriate thermal protection system.

5. Conclusions

The constant flux synchronous motor concept (CFSM) is a breakthrough technology that eliminates several of the inherent limiting factors of conventional electromagnetic launchers. The traveling-wave constant-flux environment eliminates the speed limitation introduced by heating of the projectile, since the projectile's currents are sustained by superconductors operating in persistent mode. No brushes or external power supplies are needed, eliminating the complex contact phenomena at high speeds. The CFSM principle provides contact-free propulsion and self-centering suspension forces. Projectile stabilization is aided by spinning in a low-pressure environment during launch. Experimental qualifications have been suggested that will allow testing the CFSM principle and open the way to design of practical, high-performance hypersonic electromagnetic launchers.

6. References

[1] Palmer, M. R., Dabiri, A. E., "Electromagnetic Space Launch: A Re-Evaluation in Light of Current Technology and Launch Needs and Feasibility of a Near Term Demonstration," *IEEE Transactions on Magnetics*, Vol. 25, No. 1, January 1989.

[2] Rice, E. E., Miller, L. A., Earhart, R. W., "Final Technical Report on Preliminary Feasibility Assessment for Earth-To-Space Electromagnetic Railgun Launchers," NASA Final Technical Report NAS3-22882, June 30, 1982.

[3] Dave, V. R, Goodman, D. L., Eager, T. W., Russell, K. C., "High Energy Electron Beam Welding and Materials Processing."

[4] http://www.inspacepropulsion.com/nra3.html

[5] http://www.ultramet.com/u2000tps.htm

[6] McNab, I. R.: "Launch to Space With an Electromagnetic Railgun," *IEEE Transactions on Magnetics,* Vol.39, No.1, Jan 2003.

[7] J. de Boeij, M. Steinbuch and H. Gutiérrez: "Modelling the Electromechanical Interactions in a Null-Flux EDS Maglev System," *IEEE Transactions on Magnetics,* Vol.41, No.1, Jan 2005.

[8] J. de Boeij, M. Steinbuch and H. Gutiérrez: "Mathematical Model of the 5-DOF Sled Dynamics of an Electrodynamic Maglev System with a Passive Sled," *IEEE Trans. on Magnetics,* Vol.41, No.1, Jan 2005.

[9] E. R. Laithwaite: "Induction coil guns for hypervelocities," *IEE Proceedings in Electric Power Applications,* Vol. 142, No. 3, May 1995.

[10] E. R. Laithwaite, "Adapting a linear induction motor for the acceleration of large masses to high velocities," *IEE Proceedings in Electric Power Applications,* Vol. 142, No. 4, J u l y 1995.

[11] R. J. Kaye, E. L. Brawley, W. Duggin, E. C. Cnare, D. C. Rovang, M. M. Widner: "Design and Performance of a multi-stage cylindrical reconnection launcher," *IEEE Trans. on Magnetics,* Vol. 27, No. 1, Jan 1991.

[12] M. Cowan: "A Momentum Limit for Electromagnetic Railguns," *IEEE Transactions on Magnetics,* Vol. 29, No. 1, Jan 1993.

[13] R. J. Kaye: "Operational Requirements and Issues for Coilgun Electromagnetic Launchers." *IEEE Transactions on Magnetics,* Vol. 41, No. 1, Jan 2005.